

## Scaling of the disorder operator at $(2+1)d$ U(1) quantum criticality

Yan-Cheng Wang<sup>1</sup>, Meng Cheng<sup>2,\*</sup>, and Zi Yang Meng<sup>3,†</sup>

<sup>1</sup>*School of Materials Science and Physics, China University of Mining and Technology, Xuzhou 221116, China*

<sup>2</sup>*Department of Physics, Yale University, New Haven, Connecticut 06520-8120, USA*

<sup>3</sup>*Department of Physics and HKU-UCAS Joint Institute of Theoretical and Computational Physics, The University of Hong Kong, Pokfulam Road, Hong Kong SAR, China*



(Received 31 January 2021; accepted 6 August 2021; published 17 August 2021)

We study disorder operator, defined as a symmetry transformation applied to a finite region, across a continuous quantum phase transition in  $(2+1)d$ . We show analytically that, at a conformally invariant critical point with U(1) symmetry, the disorder operator with a small U(1) rotation angle defined on a rectangle region exhibits power-law scaling with the perimeter of the rectangle. The exponent is proportional to the current central charge of the critical theory. Such a universal scaling behavior is due to the sharp corners of the region and we further obtain a general formula for the exponent when the corner is nearly smooth. To probe the full parameter regime, we carry out systematic computation of the U(1) disorder parameter in the square lattice Bose-Hubbard model across the superfluid-insulator transition with large-scale quantum Monte Carlo simulations, and confirm the presence of the universal corner correction. The exponent of the corner term determined from numerical simulations agrees well with the analytical predictions.

DOI: [10.1103/PhysRevB.104.L081109](https://doi.org/10.1103/PhysRevB.104.L081109)

**Introduction.** Spontaneous symmetry breaking is a fundamental phenomenon in nature. Symmetry-preserving states without ordering are often called “disordered.” While they might appear featureless at first sight, recent advances in the classification of quantum states [1] have revealed a rich structure underlying quantum disordered phases, as condensation of extended objects, such as symmetry domain walls or field lines of emergent gauge field [1,2]. Such hidden structures completely escape the grasp of local measurement, and non-local observables sensitive to the physics of extended objects must be exploited. A well-known example is the disorder operator in classical or quantum Ising models [3,4], which takes on a finite expectation value in the disordered phase. In the dual description, the disorder operator becomes the Wilson loop operator in a  $\mathbb{Z}_2$  gauge theory [5], which is able to distinguish confined and deconfined phases. In a closely related line of development, generalized global symmetries, known as “higher-form” symmetries [6–10], have been introduced as a general theoretical framework to systematically organize nonlocal observables. They offer new perspectives to quantum phases of matter that bridge the Landau-Ginzburg-Wilson paradigm of spontaneous symmetry breaking and more exotic phenomena of topological order.

While extended observables (and the related higher-form symmetries) have already found numerous conceptual applications, more quantitative aspects, such as their scaling at quantum criticality above  $(1+1)d$ , are still not systematically understood. Recently, the Ising disorder operator, which serves as the order parameter of a  $\mathbb{Z}_2$  1-form symmetry, was

computed by quantum Monte Carlo (QMC) simulation at the  $(2+1)d$  Ising transition [11] and new universal scaling behavior was identified. It is important to understand the generality of these features in the broad context of quantum criticality, and the relation between the universal feature to intrinsic CFT data.

In this Letter, we make progress towards answering these questions. We show that the logarithmic corner correction (to be defined below) to the disorder operator is generally present in U(1) CFTs in  $(2+1)d$ , and the universal coefficient can be related to the current central charge in the limit when the associated U(1) transformation is close to the identity. We then compare these results with unbiased QMC simulations of the disorder parameter across the superfluid-insulator transition in a Bose-Hubbard model, the prototypical example of continuous symmetry breaking transition. We find that as expected the disorder operator obeys the perimeter law in the insulating phase, and acquires a multiplicative logarithmic violation in the superfluid phase. At the critical point, we compute the corner correction and confirm the analytical predictions in the limit of small U(1) rotation angle. For more general CFTs, we derive the universal corner correction near the smooth corner limit, which is controlled by intrinsic defect CFT data.

**Disorder operator.** Let us start from general considerations. For a  $(2+1)d$  quantum lattice system with U(1) symmetry, we define a disorder operator in the following way: suppose the U(1) symmetry transformations are implemented by  $U(\theta) = \prod_{\mathbf{r}} e^{i\theta n_{\mathbf{r}}}$ , where  $n_{\mathbf{r}}$  is the charge on site  $\mathbf{r}$ . For a region  $M$ , we define

$$X_M(\theta) = \prod_{\mathbf{r} \in M} e^{i\theta n_{\mathbf{r}}}. \quad (1)$$

\*m.cheng@yale.edu

†zymeng@hku.hk

The disorder parameter is the expectation value  $\langle X_M(\theta) \rangle$  on the ground state. We note that the definition can be straightforwardly adapted to other symmetry groups [9,11].

*Scaling of the disorder parameter.* Next we discuss the scaling behavior of  $X_M(\theta)$  in various phases of the Bose-Hubbard model, especially the dependence on the geometry of  $M$ . In an insulating phase,  $\langle X_M(\theta) \rangle$  is expected to obey a perimeter law  $|\langle X_M(\theta) \rangle| \sim e^{-a_1(\theta)l}$ , where  $l$  is the perimeter of the region  $M$ . The perimeter dependence in this case can be absorbed into a local boundary term in the definition of the operator  $X_M(\theta)$ , and after the redefinition  $|\langle X_M(\theta) \rangle|$  is finite for arbitrarily large  $M$  [12]. In the superfluid phase, on the other hand, it was found in Ref. [13] that  $|\langle X_M(\theta) \rangle| \sim e^{-b(\theta)l \ln l}$ , a weaker decay than the area law for a discrete symmetry breaking state, but still cannot be remedied by any local counterterm on the boundary of  $M$ . In this sense, the disorder operator serves as an “order parameter” for the disordered (i.e., insulating) phase [4,14].

We now focus on the disorder parameter in a quantum critical state described by a CFT at low energy. Previous studies of the  $(2+1)d$  Ising CFT and other gapless critical field theories [15] suggest that  $\ln |\langle X_M(\theta) \rangle|$  takes the following form for a rectangle region:

$$\ln |\langle X_M(\theta) \rangle| = -a_1 l + s \ln l + a_0. \quad (2)$$

Here the dependence on  $\theta$  for the coefficients is suppressed. The logarithmic correction, which translates into a power law  $l^s$  in  $|\langle X_M \rangle|$ , originates from sharp corners of the region. In general  $s$  is a universal function of both  $\theta$  and the opening angle(s) of the corners (all  $\pi/2$  in this case) [16]. We conjecture that the corner correction is a generic feature for disorder operators in any  $(2+1)d$  CFT. Below we present analytical arguments to support the conjecture and also connect the universal coefficient  $s$  to intrinsic CFT data.

The first argument works for any CFT with global U(1) symmetry in the limit  $\theta \rightarrow 0$ . For small  $\theta$ , the Taylor expansion of  $X_M(\theta)$  to  $\theta^2$  order is given by

$$\langle X_M(\theta) \rangle \approx 1 - \frac{\theta^2}{2} \int_M d^2\mathbf{r}_1 \int_M d^2\mathbf{r}_2 \langle n(\mathbf{r}_1) n(\mathbf{r}_2) \rangle. \quad (3)$$

Here  $n(\mathbf{r})$  is the charge density in the continuum limit, and without loss of generality we assume  $\langle n(\mathbf{r}) \rangle = 0$ , so the first-order correction in the expansion vanishes. It is well known that, in a CFT with U(1) symmetry, the two-point function of the conserved charge density takes the following universal form:

$$\langle n(\mathbf{r}_1) n(\mathbf{r}_2) \rangle = -\frac{C_J}{(4\pi)^2} |\mathbf{r}_1 - \mathbf{r}_2|^{-4}. \quad (4)$$

Here  $C_J$  is the current central charge of the CFT, which is proportional to the universal dc conductivity  $\sigma = \frac{\pi}{16} C_J$  [17]. We can now evaluate Eq. (3) for  $M$  a  $L \times L$  square region. The integral has UV divergence, and once regularized we obtain

$$\langle X_M(\theta) \rangle \approx 1 - \frac{\theta^2 C_J}{(4\pi)^2} \left[ \left(1 + \frac{\pi}{2}\right) \frac{l}{8\delta} - \ln \frac{l}{\delta} \right], \quad (5)$$

where  $\delta$  is a short-distance cutoff. Details of the evaluation of the integral in Eq. (3) can be found in the Supplemental

Material (SM) [18]. Therefore, we find

$$s(\theta) \approx \frac{C_J}{(4\pi)^2} \theta^2, \quad \theta \rightarrow 0. \quad (6)$$

One can also show that such logarithmic correction is absent when  $M$  is a disk.

We now turn to disorder operators in a generic CFT. The universal coefficient  $s$  is generally a function of the opening angle(s) of the corners of the region  $M$ . In the previous case of a square  $M$ , there are four corners with opening angle  $\pi/2$ . We now focus on the contribution from one corner, whose opening angle  $\alpha$  is close to  $\pi$  (so the corner is nearly smooth). Under a generally accepted assumption about RG flow of defect lines in a CFT we have the following formula:

$$s(\alpha) = \frac{C_D}{12} (\pi - \alpha)^2, \quad \alpha \rightarrow \pi. \quad (7)$$

Here  $C_D$  is the defect central charge, a universal quantity for the disorder operator [see the SM [18] for the definition of  $C_D$  and the derivation of Eq. (7)] [19,20]. A very similar relation was known for entanglement entropy in CFTs [21–26], and the derivations follow essentially the same idea. We stress the generality of Eq. (7), which holds for any disorder parameter in  $(2+1)d$  CFTs.

While Eq. (6) and Eq. (7) are valid only for small parameter regimes, they provide strong evidence that the logarithmic corner corrections are universally present. In the following section we perform a systematic study of  $|\langle X_M(\theta) \rangle|$  in a U(1) boson lattice model with unbiased QMC computation and verify the analytical result of Eq. (6). We leave the lattice study of Eq. (7) for future works.

*Superfluid-insulator transition.* While the field-theoretical approach has yielded general results about universal features of the disorder parameter, one has to take various limits, e.g.,  $\theta \rightarrow 0$ , to make progress analytically. To probe parameter regimes where analytical results are not available, we turn to numerical simulations.

We consider the Bose-Hubbard model on the square lattice, which provides a concrete realization of the superfluid-insulator transition [27]. The Hamiltonian takes the following standard form:

$$H = -t \sum_{\langle ij \rangle} (b_i^\dagger b_j + \text{H.c.}) + \frac{U}{2} \sum_i n_i(n_i - 1) - \mu \sum_i n_i, \quad (8)$$

where  $b^\dagger(b)$  is the boson creation (annihilation) operator,  $n_i = b_i^\dagger b_i$  is the boson number,  $t > 0$  is the hopping between nearest-neighbor sites on the square lattice,  $U > 0$  is the on-site repulsion, and  $\mu$  is the chemical potential. We set  $t = 1$  as the unit of energy for convenience.

The ground state of this model has two phases: a Mott insulator (MI) phase for large  $U/t$  and a superfluid (SF) phase for small  $U/t$ , separated by a continuous phase transition. At integer filling, the transition belongs to the 3D XY universality class, also known as the O(2) Wilson-Fisher theory [27]. For  $\langle n \rangle = 1$ , the critical point is located at  $U_c/t = 16.7424(1)$ ,  $\mu/t = 6.21(1)$ , determined from previous works [28–30].

*Numerical results.* We choose the region  $M$  to be a  $R \times R$  square region in the lattice, with perimeter  $l = 4R - 4$ . For an illustration, see Fig. 1. To calculate the disorder operator

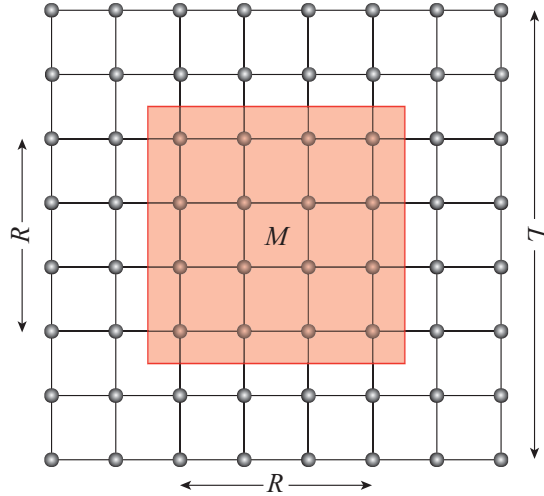


FIG. 1. Disorder operator  $X_M$  applied on regions with size  $R \times R$  and perimeter  $l = 4R - 4$  in the  $L \times L$  square lattice of Boson-Hubbard model.

of the Bose-Hubbard model, we employ large-scale stochastic series expansion QMC simulations [31–33], and compute the expectation value of  $X_M(\theta)$  on a finite lattice with  $L = \beta = 1/T$  and  $R \in [1, L/2]$  to access the thermodynamic limit. For the MI and SF phases we fix  $\theta = \frac{\pi}{2}$ .

First, in the MI phase the disorder parameter decays according to the perimeter law. This is shown in Fig. 2, where, in a semilog plot, the relation  $|\langle X_M(\frac{\pi}{2}) \rangle| \sim e^{-a_1 l}$  is clearly seen. We also observe that the coefficient  $a_1$  decreases monotonically with  $U$  from  $U = 17$  to  $26$ , as shown in the inset of Fig. 2, consistent with the theoretical expectation.

Inside the SF phase, the disorder parameter decays more rapidly with the perimeter  $l$ , as depicted in Fig. 3. We find that the data in Fig. 3 can be well fitted by the function  $|\langle X_M(\frac{\pi}{2}) \rangle| \sim e^{-b l \ln \frac{l}{c}}$ . Interestingly, the coefficient  $b$  extracted from the fit is proportional to the superfluid stiffness  $\rho_s$  =

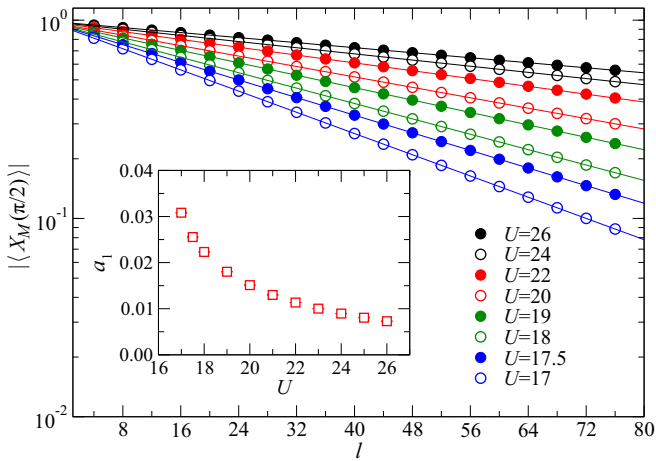


FIG. 2. Disorder operator  $|\langle X_M(\theta = \frac{\pi}{2}) \rangle|$  as function of  $l$  in the MI phase (from  $U = 17$  to  $U = 26$ ) with system sizes up to  $L = 40$  and  $R \in [1, L/2]$ . Dots are the QMC results with error bars smaller than the symbol size and the solid lines are the fitting with function  $e^{-a_1 l}$ . Inset shows the obtained  $a_1$  as a function of  $U$ .

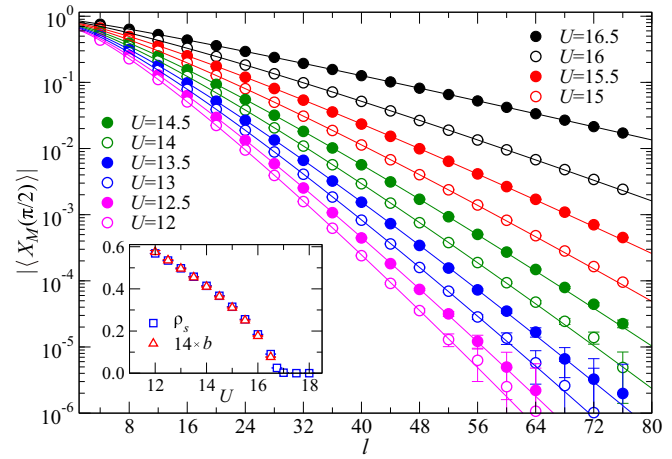


FIG. 3. Disorder operator  $|\langle X_M(\theta = \frac{\pi}{2}) \rangle|$  as function of  $l$  in the SF phase (from  $U = 16.5$  to  $U = 12.0$ ) with system sizes up to  $L = 40$  and  $R \in [1, L/2]$ . Dots are the QMC results with error bars smaller than the symbol size and the solid lines show the fit with function  $e^{-b l \ln \frac{l}{c}}$ . Inset shows the fitting parameter  $b$  as a function of  $U$  as well as the superfluid stiffness  $\rho_s$  for the same parameter sets.

$(W_x^2 + W_y^2)/(4\beta t)$  (where  $W_{x,y}$  is the winding number along  $x$  or  $y$  direction), inside the SF phase (shown in the inset of Fig. 3), also consistent with theoretical analysis [13].

We now turn to the critical point  $U = U_c = 16.7424$ . Numerical results of  $\langle X_M(\theta) \rangle$  as a function of  $l$  for various values of  $\theta$  are shown in Fig. 4, and we find that the data can be fitted with the scaling form in Eq. (2) with good quality, in that the coefficient of the subleading logarithmic term  $s$ , as shown in the inset of Fig. 4, clearly manifests a quadratic dependence with respect to  $\theta$ , when  $\theta$  is small. However, one might worry

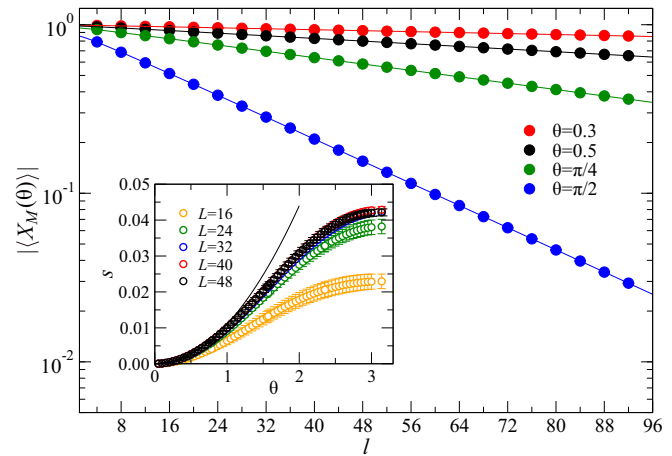


FIG. 4. Disorder parameter  $|\langle X_M(\theta) \rangle|$  as function of  $l$  at the critical point ( $U_c = 16.7424$ ) with  $\theta = 0.3, 0.5, \pi/4, \pi/2$  and system sizes up to  $L = 48$ ,  $R \in [1, L/2]$ . Dots are the QMC results with error bars smaller than the symbol size and the solid lines show the fit by the function in Eq. (2). Inset shows the  $\theta$  dependence of universal coefficient  $s$  for different system sizes. For small  $\theta$ , a quadratic dependence clearly manifests. The finite-size results converge for  $L = 40, 48$  and fitting with Eq. (6) yields the coefficient  $\frac{s}{\theta^2} \approx 0.011(1)$ , close to the exact value  $\frac{C_J}{(4\pi)^2} = 0.01145$ .

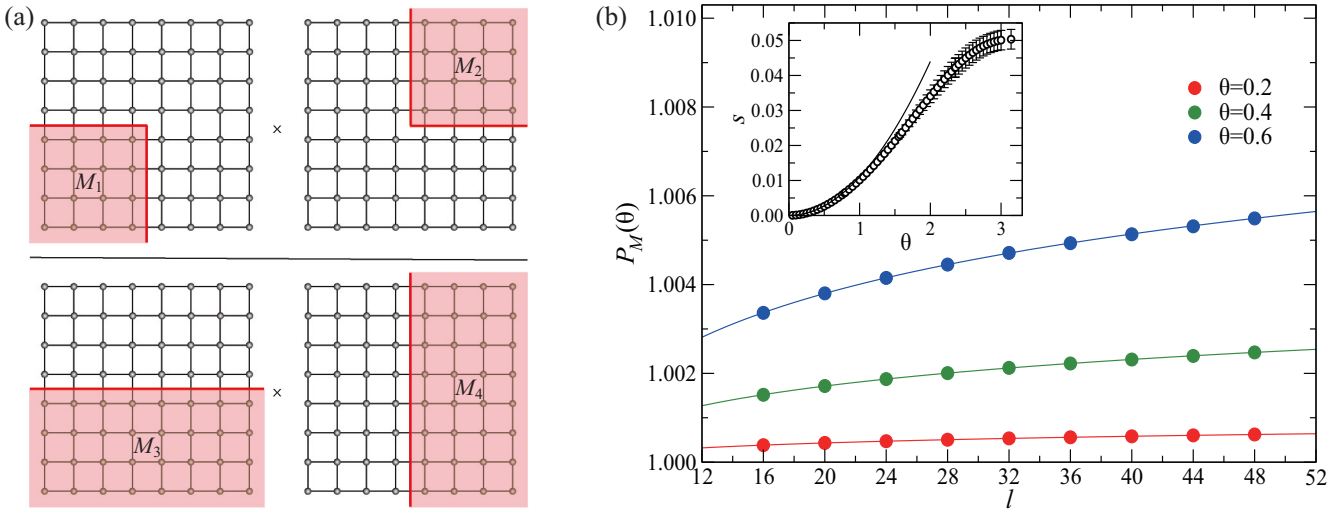


FIG. 5. (a) Regions  $M_1$ ,  $M_2$ ,  $M_3$ , and  $M_4$  used to determine the corner contribution in Eq. (2) on the square lattice with open boundary condition, and the perimeter of  $M_1 \cup M_2$  is equal to that of  $M_3 \cup M_4$ . (b)  $P_M(\theta)$  as function of  $l=L$  at the critical point ( $U_c = 16.7424$ ) with the system size  $L = 16, 20, 24, 28, 32, 36, 40, 44, 48$ . The data points are fitted by  $l^{s(\theta)/2}$  for each  $\theta$ , as shown by the solid lines in the main panel, to obtain  $s(\theta)$  for  $\theta \in [0, \pi]$  denoted by the black dots in the inset. Then fitting  $s(\theta)$  with  $\frac{C_J}{(4\pi)^2} \theta^2$  for  $\theta \in [0, 0.3]$ , one finds  $\frac{C_J}{(4\pi)^2} \approx 0.0109(5)$ . The solid line in the inset shows the fit.

whether such fitting can reliably extract the coefficient  $s$  of the subleading logarithmic term, as the perimeter contribution clearly dominates.

We thus apply a different method adapted from Ref. [34] to directly extract the corner correction. In this approach, we work on a  $L \times L$  square lattice with open boundaries. We measure disorder parameters for each of the four regions  $M_{1,2,3,4}$  as shown in Fig. 5(a). The regions are chosen such that the perimeter of  $M_1 \cup M_2$  is equal to that of  $M_3 \cup M_4$ . So the following combination

$$P_M(\theta) = \left| \frac{\langle X_{M_1}(\theta) \rangle \langle X_{M_2}(\theta) \rangle}{\langle X_{M_3}(\theta) \rangle \langle X_{M_4}(\theta) \rangle} \right| \quad (9)$$

cancels the leading term  $a_1 l$  in Eq. (2). Since both  $M_1$  and  $M_2$  contain one  $\pi/2$  corner, we expect  $P_M(\theta) \sim l^{s(\theta)/2}$ , which can then be used to determine  $s(\theta)$ . We find that the two methods give basically identical values of  $s$  for small  $\theta$ , although there are small discrepancies when  $\theta$  gets close to  $\pi$ . The full function  $s(\theta)$  for  $\theta \in [0, \pi]$  determined from the latter method is shown in the inset of Fig. 5(b), which is very close to the function:  $0.047 \sin^2(\frac{\theta}{2})$ .

To corroborate the analytical results, we examine more closely the function  $s(\theta)$  as  $\theta \rightarrow 0$ . As shown in the insets of Figs. 4 and 5,  $s(\theta)$  exhibits a clear  $\theta^2$  dependence, and the coefficient is found to be  $0.011(1)$  for the direct fitting method (Fig. 4) and  $0.0109(5)$  for the second method (Fig. 5). Using the formula Eq. (6) and the best estimate  $C_J = 1.8088$  for the O(2) Wilson-Fisher CFT [30,35–37], we obtain the theoretical value for the proportionality constant  $\frac{C_J}{(4\pi)^2} = 0.01145$ . The numerical results agree quite well with the theory.

*Discussions.* We briefly discuss future directions. An immediate question is to verify the smooth corner limit Eq. (7) in a lattice model, which would provide a way to extract the defect central charge. We have mainly considered the modulus

of the disorder parameter  $\langle X_M \rangle$ . An interesting question is to understand the phase of  $\langle X_M \rangle$  and how it depends on intrinsic CFT data. According to the small  $\theta$  expansion, the leading imaginary part appears at  $\theta^3$  order, which is then related to the three-point function of the density operator.

In summary, we develop a computational and theoretical toolkit about nonlocal observables—the disorder operator—and the associated higher-form symmetry in the lattice model of quantum many-body systems, and demonstrate that it can directly reveal the CFT data of the critical point beyond the conventional local observables. This offers a different concept and technique in understanding an aspect of phase transitions. It would be interesting to study other conformal field theories, such as O( $n$ ) symmetry-breaking transitions [38,39] and even more unconventional phase transitions such as the deconfined quantum critical points [40–43] or nonconformal scale-invariant theories such as the Lifshitz critical point [44].

*Note added.* We would like to draw the reader's attention to a closely related work by Wu, Jian, and Xu [45] in the same arXiv listing. We also have become aware of an upcoming work by Estienne, Stéphan, and Witczak-Krempa on related topics [46].

*Acknowledgments.* We would like to thank W. Witczak-Krempa and S.-H. Shao for stimulating discussions which benefited the present work, as well as comments on the first draft. We are grateful for C.-M. Jian and C. Xu for correspondence and sharing unpublished work. Y.C.W. acknowledges the support from the NSFC under Grants No. 11804383 and No. 11975024, the NSF of Jiangsu Province under Grant No. BK20180637, and the Fundamental Research Funds for the Central Universities under Grant No. 2018QNA39. M.C. acknowledges support from the NSF under Award No. DMR-1846109 and the Alfred P. Sloan foundation. Z.Y.M. acknowledges support from the RGC of Hong Kong SAR of China (Grants No. 17303019,

No. 17301420, and No. AoE/P-701/20), MOST through the National Key Research and Development Program (Grant No. 2016YFA0300502), and the Strategic Priority Research Program of the Chinese Academy of Sciences (Grant No. XDB33000000). We thank the Computational Initiative at the Faculty of Science and the Information Technology

Services at the University of Hong Kong and the Tianhe platforms at the National Supercomputer Centers in Tianjin and Guangzhou for their technical support and generous allocation of CPU time. We also acknowledge Beijng PARATERA Tech CO., Ltd. [47] for providing HPC resources that have contributed to the research results reported within this Letter.

---

[1] X.-G. Wen, *Rev. Mod. Phys.* **89**, 041004 (2017).

[2] X.-G. Wen, *Science* **363**, eaal3099 (2019).

[3] L. P. Kadanoff and H. Ceva, *Phys. Rev. B* **3**, 3918 (1971).

[4] E. Fradkin, *J. Stat. Phys.* **167**, 427 (2017).

[5] F. Wegner, *J. Math. Phys.* **12**, 2259 (1971).

[6] Z. Nussinov and G. Ortiz, *Proc. Natl. Acad. Sci. USA* **106**, 16944 (2009).

[7] Z. Nussinov and G. Ortiz, *Ann. Phys. (NY)* **324**, 977 (2009).

[8] D. Gaiotto, A. Kapustin, N. Seiberg, and B. Willett, *J. High Energy Phys.* **02** (2015) 172.

[9] W. Ji and X.-G. Wen, *Phys. Rev. Research* **2**, 033417 (2020).

[10] L. Kong, T. Lan, X.-G. Wen, Z.-H. Zhang, and H. Zheng, *Phys. Rev. Research* **2**, 043086 (2020).

[11] J. Zhao, Z. Yan, M. Cheng, and Z. Y. Meng, *Phys. Rev. Research* **3**, 033024 (2021).

[12] M. B. Hastings and X.-G. Wen, *Phys. Rev. B* **72**, 045141 (2005).

[13] E. Lake, [arXiv:1802.07747](https://arxiv.org/abs/1802.07747).

[14] M. Levin, *Commun. Math. Phys.* **378**, 1081 (2020).

[15] X.-C. Wu, W. Ji, and C. Xu, *J. Stat. Mech.* (2021) 073101.

[16] Similar corner contributions were known to exist for Renyi entropy in a CFT, which can be understood as the disorder parameter of the replica symmetry.

[17] M. P. A. Fisher, G. Grinstein, and S. M. Girvin, *Phys. Rev. Lett.* **64**, 587 (1990).

[18] See Supplemental Material at <http://link.aps.org/supplemental/10.1103/PhysRevB.104.L081109>, where we give details of the evaluation of the integral in Eq. (3) and present a field-theoretical derivation of the corner contribution in the smooth limit.

[19] M. Billó, M. Caselle, D. Gaiotto, F. Gliozzi, M. Meineri, and R. Pellegrini, *J. High Energy Phys.* **07** (2013) 055.

[20] D. Gaiotto, D. Mazac, and M. F. Paulos, *J. High Energy Phys.* **03** (2014) 100.

[21] H. Casini and M. Huerta, *Nucl. Phys. B* **764**, 183 (2007).

[22] P. Bueno, R. C. Myers, and W. Witczak-Krempa, *J. High Energy Phys.* **09** (2015) 091.

[23] P. Bueno and R. C. Myers, *J. High Energy Phys.* **08** (2015) 068.

[24] T. Faulkner, R. G. Leigh, and O. Parrikar, *J. High Energy Phys.* **04** (2016) 088.

[25] L. Bianchi, M. Meineri, R. C. Myers, and M. Smolkin, *J. High Energy Phys.* **07** (2016) 076.

[26] W. Witczak-Krempa, *Phys. Rev. B* **99**, 075138 (2019).

[27] M. P. A. Fisher, P. B. Weichman, G. Grinstein, and D. S. Fisher, *Phys. Rev. B* **40**, 546 (1989).

[28] B. Capogrosso-Sansone, S. G. Söyler, N. Prokof'ev, and B. Svistunov, *Phys. Rev. A* **77**, 015602 (2008).

[29] S. G. Söyler, M. Kiselev, N. V. Prokof'ev, and B. V. Svistunov, *Phys. Rev. Lett.* **107**, 185301 (2011).

[30] K. Chen, L. Liu, Y. Deng, L. Pollet, and N. Prokof'ev, *Phys. Rev. Lett.* **112**, 030402 (2014).

[31] O. F. Syljuåsen and A. W. Sandvik, *Phys. Rev. E* **66**, 046701 (2002).

[32] A. W. Sandvik, *Computational Studies of Quantum Spin Systems*, AIP Conf. Proc. No. 1297 (AIP, Melville, NY, 2010), p. 135.

[33] Z. Y. Meng and S. Wessel, *Phys. Rev. B* **78**, 224416 (2008).

[34] A. B. Kallin, E. M. Stoudenmire, P. Fendley, R. R. P. Singh, and R. G. Melko, *J. Stat. Mech.* (2014) P06009.

[35] W. Witczak-Krempa, E. S. Sørensen, and S. Sachdev, *Nat. Phys.* **10**, 361 (2014).

[36] E. Katz, S. Sachdev, E. S. Sørensen, and W. Witczak-Krempa, *Phys. Rev. B* **90**, 245109 (2014).

[37] S. M. Chester, W. Landry, J. Liu, D. Poland, D. Simmons-Duffin, N. Su, and A. Vichi, *J. High Energy Phys.* **06** (2020) 142.

[38] M. Lohöfer, T. Coletta, D. G. Joshi, F. F. Assaad, M. Vojta, S. Wessel, and F. Mila, *Phys. Rev. B* **92**, 245137 (2015).

[39] N. Ma, P. Weinberg, H. Shao, W. Guo, D.-X. Yao, and A. W. Sandvik, *Phys. Rev. Lett.* **121**, 117202 (2018).

[40] T. Senthil, L. Balents, S. Sachdev, A. Vishwanath, and M. P. A. Fisher, *Phys. Rev. B* **70**, 144407 (2004).

[41] Y. Q. Qin, Y.-Y. He, Y.-Z. You, Z.-Y. Lu, A. Sen, A. W. Sandvik, C. Xu, and Z. Y. Meng, *Phys. Rev. X* **7**, 031052 (2017).

[42] C. Wang, A. Nahum, M. A. Metlitski, C. Xu, and T. Senthil, *Phys. Rev. X* **7**, 031051 (2017).

[43] Y.-C. Wang, N. Ma, M. Cheng, and Z. Y. Meng, Scaling of disorder operator at deconfined quantum criticality, [arXiv:2106.01380](https://arxiv.org/abs/2106.01380) [cond-mat.str-el].

[44] E. Fradkin and J. E. Moore, *Phys. Rev. Lett.* **97**, 050404 (2006).

[45] X.-C. Wu, C.-M. Jian, and C. Xu, Universal Features of Higher-Form Symmetries at Phase Transitions, [arXiv:2101.10342](https://arxiv.org/abs/2101.10342) [cond-mat.str-el].

[46] B. Estienne, J.-M. Stéphan, and W. Witczak-Krempa, Cornering the universal shape of fluctuations, [arXiv:2102.06223](https://arxiv.org/abs/2102.06223) [cond-mat.str-el].

[47] <https://paratera.com/>.